Indian J. Phys. **78(8)**, 733-737 (2004)

AN INTERNATIONAL JOURNAL
IJP

Investigation of tin-incorporated nanocomposite diamond like carbon film

S Kundoo, P Saha and K K Chattopadhyay*
Department of Physics, Jadavpur University, Kolkata-700 032, India

E-mail : kkc@juphys.cmet.in

Abstract : Semiconducting Sn-incorporated nanocomposite diamond like carbon (Sn-DLC) films were synthesized by DC plasma-enhanced chemical vapour deposition (PECVD) method using $SnCl_2.2H_2O$ salt dissolved in methanol solution as the doping source and acetylene as the carrier gas. Fourier transform infrared spectroscopy (FTIR) measurements showed different vibrational modes of tetrahedrally bonded carbon and also some small peaks due to Sn-C bonding vibrations. Transmission electron microscopy (TEM) image and electron diffraction pattern also confirmed the incorporation of nanocrystalline Sn particles into the amorphous DLC matrix. Due to presence of Sn clusters optical band gap of the films decreased sharply compared to the intrinsic material. It was found that resistivity of Sn-incorporated DLC films decreased drastically by eight orders of magnitude than that of the undoped DLC film. Also the films exhibited good field emission properties at lower turn-on field.

Keywords : Diamond like carbon, nanocomposite, TEM, field emission.

PACS Nos. : 81.15.Gh, 73.61.-r, 79.70.+q

1. Introduction

Diamond like carbon (DLC) can be defined as a metastable phase of a-C or a-C:H containing a significant fraction of sp^3 hybridization which govern the mechanical properties of the material. As well, it is commonly accepted that the graphitic sp^2 clusters are embedded in the amorphous sp^3 bonded matrix, where the collective behavior of sp^2 sites is responsible for the optical and electrical properties. However, amorphous DLC has aroused immense interest among scientists all over the world over the last two decades, as it is an inexpensive alternative to diamond for many industrial applications due to its diamond like properties. These properties include high mechanical hardness, dielectric strength, chemical inertness, low wear and friction, optical transparency in the visible and infrared region, high electrical resistivity, high thermal conductivity and negative electron affinity. Instead of these interesting properties, DLC films have several known limitations such as high internal stress and low thermal stability. The high intrinsic stress generated in the film causes some serious problems in various applications of this material, like degradation of electrical and optical properties and often causes delamination of the films from the substrate.

A large number of different techniques have evolved for the deposition of amorphous diamond like carbon films during the last two decades, the majority of the techniques reported so far involved chemical vapor deposition [1,2]. Also various attempts have been made to dope a:DLC films with different elements such as nitrogen [3], iodine [4], boron, phosphorous, fluorine *etc.* and their doping effects on the electrical, optical and mechanical properties of DLC films have been extensively investigated. It has been shown that the range of technical applications of the DLC films can be greatly enhanced by doping them with metal elements [5]. Metal incorporated DLC films (Me-C:H) have attracted significant attention in the past few years due to their better adhesion and tribological properties compared to the pure diamond like carbon films. These films are also

*Corresponding Author

found to exhibit interesting electrical properties, with their conductivities varied over many orders of magnitude with the addition of a small fraction of metal element [6]. To date, several techniques have been proposed for the deposition of Me-C:H films using various metallic elements (*e.g.* Au, Ta, Ti, Li, Sn, Mo *etc.*) as dopants, the most common of which include sputter deposition in a hydrocarbon and Ar gas mixture [7], RF plasma enhanced chemical vapor deposition [8].

In this paper, we report the synthesis of highly conducting Sn-incorporated a:DLC (Sn-DLC) films by DC plasma enhanced chemical vapor deposition. Structural, optical and electrical characterization of the films along with their field emission properties were also carried out.

2. Experimental

Our deposition apparatus was a conventional vacuum system equipped with rotary and diffusion pumps. The vacuum chamber was designed with appropriate stainless steel (SS) vacuum couplings through which different feed-throughs like vacuum port, pressure gauge, gas mixture inlets, thermocouple *etc.* could be introduced. The plasma was produced between two parallel plate SS electrodes. The lower disc was grounded upon which the substrate was placed. The upper disc was used as the cathode electrode. When chamber pressure attained 10^{-5} mbar, then C_2H_2 gas was introduced and diamond like carbon films were deposited at a pressure of 0.4 mbar. Silicon and glass substrates were used. Deposition was made at 2.0 kV DC supply, corresponding current density was 20 mA/cm^2. Deposition time was 40 minutes. For tin doping stannous chloride ($SnCl_2.2H_2O$) dissolved in methanol solution was used. One portion of C_2H_2 gas was passed through the solution for bubble formation and then introduced into the chamber. Sn concentration was varied in the deposited film by dissolving different amounts of stannous chloride in the methanol solution.

The films were characterized by Fourier transform infrared spectroscopy (FTIR), X-ray diffraction (XRD) studies, transmission electron microscopy (TEM), UV-VIS-NIR spectrophotometry and electrical measurements.

3. Results and discussion

3.1. Fourier transform infrared spectroscopy :

IR spectroscopic studies were carried out to analyze the structure and bonding state of the deposited sample. The FTIR absorbance spectrum of a typical Sn doped DLC film deposited on Si substrate is shown in Figure 1. The

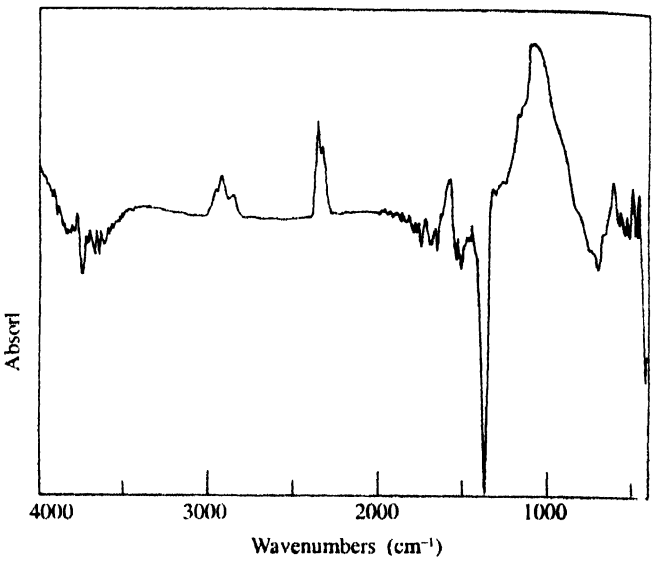

Figure 1. FTIR absorbance spectrum of a typical Sn-DLC film deposited on Si substrate.

spectrum was recorded in a FTIR spectrometer (Nicolet Magna–750) from 400 to 4000 cm^{-1} by subtracting the absorption due to the Si substrate. The spectrum shows different vibrational modes of various bonding. The band at 2923 cm^{-1} corresponds to the asymmetric $-CH_2$ stretch for a typical hydrocarbon. It can also be observed that there are asymmetric $-CH_3$ stretch mode at 2956 cm^{-1} and symmetric stretch mode at 2855 cm^{-1}. All these vibrational frequencies are typical of tetrahedrally bonded carbon (sp^3 bonding) in hydrocarbons. The peaks in the range of 1325-1600 cm^{-1} are assigned to vibrations due to sp^2 carbon bonding. The small absorption peaks around 454–565 cm^{-1} can be assigned with Sn-C bonding vibrations.

3.2. Structural characterization :

The deposited films were characterized by X-ray diffraction (XRD) technique using a diffractometer (Philips PW 1730/10) by Cu K_α line operating at 30 kV, 20 mA with a normal $\theta - 2\theta$ scanning. The films deposited on glass, as well as on Si (400) substrates showed an amorphous structure (Figure not shown here).

Structural analysis was also performed using transmission electron microscopy (TEM). TEM investigations were performed on a Hitachi, H-600 microscope at an operating voltage of 50 kV. Incorporation of nanocrystalline Sn particles in the amorphous DLC

(a:DLC) matrix was confirmed in TEM studies of the films deposited on a copper grid to a thickness of about 60 nm. Figure 2(a) shows the TEM image of a representative Sn-DLC film. The bright areas are C-enriched amorphous matrix. The dark areas are most likely Sn particles with an average grain size of 30 nm in diameter. Figure 2(b) shows the selected area electron

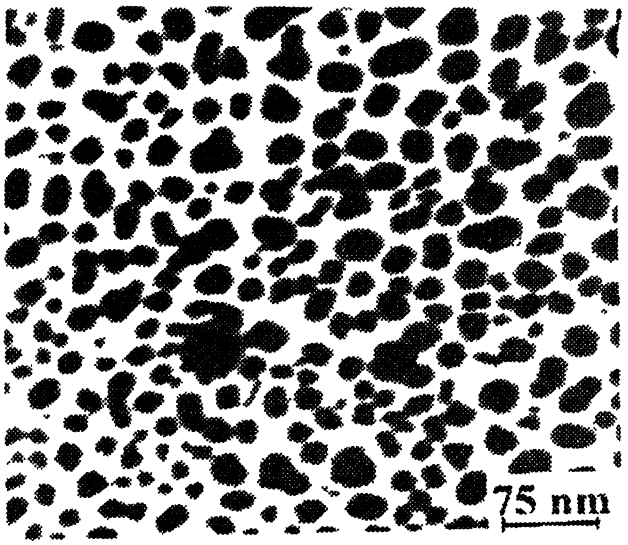

Figure 2(a). TEM image of a Sn-DLC film.

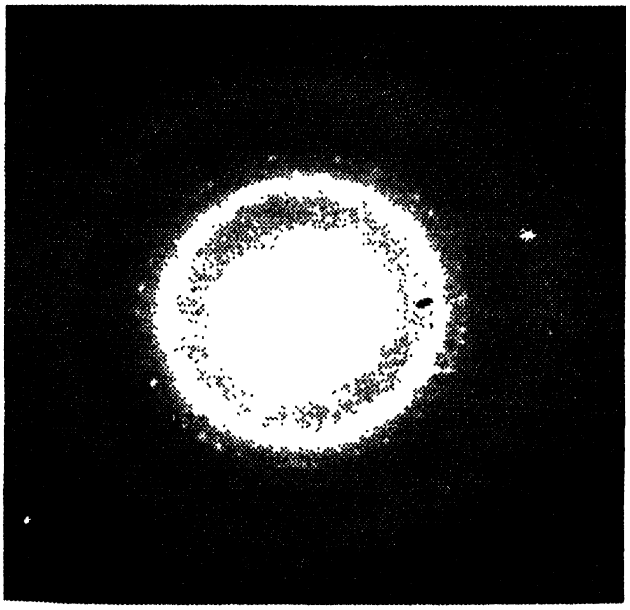

Figure 2(b). Electron diffraction pattern of the film.

diffraction (SAED) pattern of this film. The pattern shows a set of rings with characteristic spots. The diffraction rings have lattice spacings (d) with values 3.75, 2.29, 1.94 and 1.35 Å which fit very well with that of the (111), (220), (311) and (422) reflections, respectively, of the α-Sn (cubic) phase [9].

3.3. Optical absorption studies :

Optical studies were performed by measuring the transmittance of the films deposited on glass substrates in the wavelength region λ = 300–800 nm using a spectrophotometer (Hitachi-U3410) by subtracting the absorption due to the glass substrate taking as reference. It has been observed that optical transmittance was reduced in the infrared region with the increase of Sn concentration. This decrease is certainly related to the increased absorption in the presence of Sn clusters.

From the transmittance data using Manifacier model [10], absorption coefficients (α) were calculated in the region of strong absorption. In amorphous material, true band gap cannot be uniquely defined. The Tauc gap was calculated [11] by extrapolating the linear portion of the $(\alpha h\nu)^{1/2}$ *vs* $h\nu$ plot and taking the intercept on the $h\nu$ axis where $(\alpha h\nu)^{1/2} = 0$. Figure 3 shows that the Tauc gap of the film decreases sharply with the increase of Sn concentration. Sn doping changes the band structure of the DLC films.

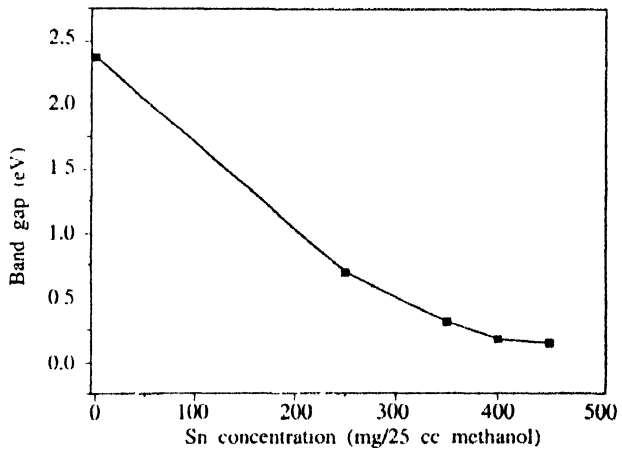

Figure 3. Variation of Tauc band gap of the films with Sn concentrations.

3.4. Electrical measurements :

The dependence of dc conductivity (σ) on temperature (T) of undoped and Sn doped amorphous DLC films were measured by Kiethley electrometer (Model 6514) in the temperature range of 300–500 K. It can be seen that the resistivity of the films decreased by eight orders of magnitude by Sn doping. The minimum resistivity obtained for our Sn-DLC films was 9.09 × 10^{-2} Ω-cm. Similar drastic changes in resistivity have also been reported for tungsten and tin incorporated amorphous carbon films [6,8]. The dc conductivity variation with temperature can be expressed in the simplest form :

$$\sigma = \sigma_0 \exp(-E_a/kT), \quad (1)$$

where E_a is the activation energy which corresponds to the energy difference between the Fermi level and conduction level, σ_0 is a temperature independent factor.

Activation energies were calculated from the slopes of the $\ln\sigma$ *vs* $1/T$ plots (not shown here). Figure 4 reveals the dependence of room temperature resistivity (ρ_{RT}) and activation energies (E_a) on doping concentrations.

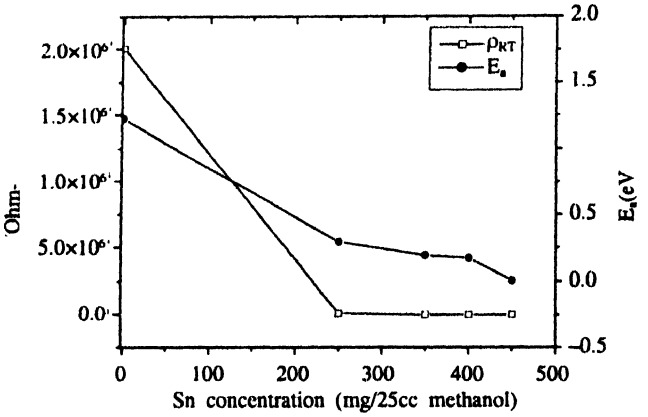

Figure 4. Room temperature resistivity and activation energies of the films deposited with different doping concentrations.

The observed thermally activated conduction behavior could be attributed to the tunnelling of electrons between the metal clusters, with the decrease in activation energy at higher Sn content.

Electron field emission properties of the films were also studied. Field emission measurements were carried out by using a parallel plate configuration with the sample mounted on the cathode and a stainless steel anode having an area of ~0.385 cm². The anode was attached to a micropositioner for varying the cathode-anode spacing with an accuracy of ±10 μm. Measurements were performed in a high vacuum of 10^{-6}–10^{-7} mbar. Figure 5 shows the emission current density (J) plotted against applied field (E) for an undoped and Sn-doped DLC films. It can be seen that upon addition of tin in the amorphous DLC matrix, the turn-on field (E_c) was reduced by about half for the Sn-incorporated DLC film than that of the film grown without tin. We define the turn-on field (E_c) as the electric field needed to get a current density of 0.5 μA/cm² and electric field was computed as E_c = applied voltage/cathode-anode spacing. The lowest turn-on field achieved was ~7.41 volt/μm for the sample with doping concentration of 500 mg $SnCl_2$ per 25 cc of methanol, while for the intrinsic material it was ~15 Volt/μm. Field emission characteristics of the films were studied using Fowler-Nordheim (F-N) theory [12]. A simplified FN equation for the local current density J (Amp/cm²) at some point on the emitting surface may be written as [12]

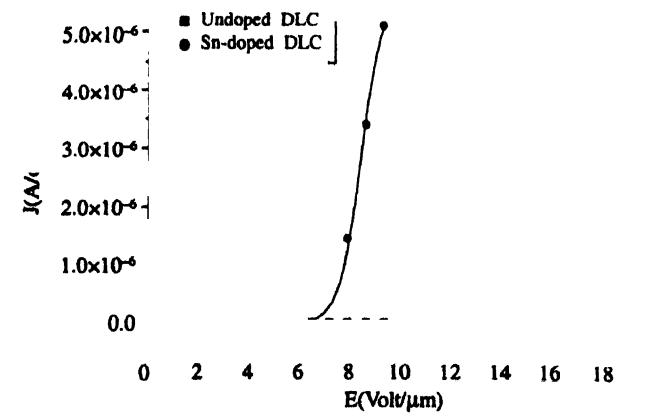

Figure 5. Emission current density against electric field from undoped and Sn-incorporated DLC films.

$$J = S\frac{1.54\times10^{2}F^{2}}{\phi}\exp\left(-6.83\times10^{3}\phi^{3/2}\right) \quad (2)$$

where F is the local field, ϕ is the local work function called the emission barrier. F is not simply V/d, which is the macroscopic field obtained with an applied voltage of V between two electrodes separated by distance d.

But in most cases, $F = \beta E$, where $E = V/d$, β is the geometrical enhancement factor defined as [13]

$$\beta = d/[kr(d-r)], \quad (3)$$

r is the radius of curvature at the tip of emitter.

k is a constant and k ~5 for a distant anode.

S is the fraction of area emitting electrons.

E is in Volt/μm.

The FN curves for Sn incorporated DLC films and the film without Sn are plotted in Figure 6. We can see that our data give a reasonable fit to eq. (3) for the applied field in the region above ~6 × 10^4 volts/cm for Sn-doped film and above ~13 × 10^4 volts/cm for the intrinsic material. The linearity of these FN plots points towards the field emission mechanism. Assuming plane flat emitter with β = 1, emission barriers (ϕ) were calculated from the slopes of FN plots. The value of ϕ was reduced from 0.06 eV to 0.0176 eV for maximum Sn incorporation in our measurement range. But, true barrier must be larger than these values. Such low work function obtained may be due to an underestimation of the field enhancement factor β. We can infer that the effective barrier height is reduced in presence of Sn clusters in the amorphous DLC matrix.

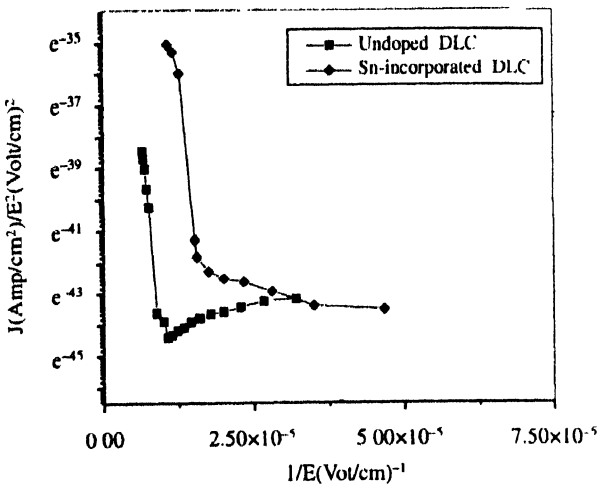

Figure 6. FN plots of undoped and Sn-doped DLC films

The details of field emission mechanism in the Sn-doped DLC films, the dependence of threshold field and emission current density on the doping level will be the topic of future publications.

4. Conclusions

Sn-incorporated nanocomposite diamonds like carbon (DLC) films have been synthesized by DC plasma-enhanced chemical vapour deposition (PECVD) method. Structure and bonding states of the deposited sample were investigated by FTIR spectroscopy. Electron diffraction pattern of the film indicated the incorporation of nanometer sized Sn particles into the amorphous DLC matrix. Optical gap and resistivity decreased sharply in the presence of Sn clusters in the films. Also, threshold field for electron emission shows a large improvement in the field emission characteristics with the incorporation of Sn into the DLC matrix.

Acknowledgments

The authors wish to thank the University Grants Commission for financial support for the work. One of the authors (SK) wishes to thank the Counsil of Scientific and Industrial Research (CSIR) for awarding her Senior research Fellowship (SRF) during the execution of the work.

References

[1] D Dutta, K K Chattopadhyay, J Dutta, S Chaudhuri and A K Pal *Mater Lett* **18** 114 (1993)

[2] S Kumar, C M S Rauthan, P N Dixit, K M K Srivatsa, M Y Khan and R Bhattacharyya *Vacuum* **63** 443 (2001)

[3] S Bhattacharyya, K Walzer, M Hietschold and F Richter *J. Appl. Phys* **89** 1184 (2001)

[4] M Allon-Alaluf and N Croitoru *Diamond Relat Mater.* **6** 555 (1997)

[5] J Robertson *Prog Solid State Chem.* **21** 199 (1991)

[6] Rusli, S F Yoon, H Yang, J Ahn, Q F Huang, Q Zhang, Y P Guo, C Y Yang, E J Teo, A T S Wee and A C H Huan *Thin Solid Films* **355-356** 174 (1999)

[7] P Canet, C Laurent, J Akinnifesi and B Despax *J. Appl. Phys* **72** 2423 (1992)

[8] Y Inoue, T Komoguchi, H Nakata and O Takai *Thin Solid Films* **322** 41 (1998)

[9] JCPDS Data Card, No -5-0390

[10] J C Manifacier, M De Murcia, J P Fillard and E Vicario *Thin Solid Films* **41** 127 (1997)

[11] J Robertson *Materials Sci. Engg (Reports)* **R37** 129(2002)

[12] R H Fowler and L W Nordheim *Proc. Roy Soc* (London) *Ser. A* **119** 173 (1928)

[13] I Brodie *Proc. IEEE* **82** 1006 (1994)